13. Kapaev V V, Kopaev Yu V *Pis'ma Zh. Eksp. Teor. Fiz.* **68** 211 (1998) [*JETP Lett.* **68** 223 (1998)]
14. Belyavskii V I, Kopaev Yu V *Pis'ma Zh. Eksp. Teor. Fiz.* **73** 87 (2001) [*JETP Lett.* **73** 82 (2001)]
15. Belyavsky V I, Kopaev Yu V *J. Supercond. Nov. Magn.* **19** 251 (2006)
16. Leggett A J *Nature Phys.* **2** 134 (2006)
17. Zaanen J et al. *Nature Phys.* **2** 138 (2006)
18. Scalapino D J *J. Supercond. Nov. Magn.* **19** 195 (2006)
19. Anderson P W *Science* **316** 1705 (2007)
20. Ginzburg V L, Maksimov E G *Physica C* **235 – 240** 193 (1994)
21. Alexandrov A S, Mott N *Polarons and Bipolarons* (Singapore: World Scientific, 1995)
22. Zhao G-M et al. *Nature* **385** 236 (1997)
23. Müller K A *J. Supercond.* **12** 3 (1999)
24. Ginzburg V L *J. Supercond.* **13** 665 (2000)
25. Kulić M L *Phys. Rep.* **338** 1 (2000)
26. Abrikosov A A, in *Superconducting and Related Oxides: Physics and Nanoengineering V* (Proc. SPIE, Vol. 4811, Eds I Bozovic, D Pavuna) (Bellingham, Wash.: SPIE, 2002) p. 1
27. Ponomarev Ya G, Maksimov E G *Pis'ma Zh. Eksp. Teor. Fiz.* **76** 455 (2002) [*JETP Lett.* **76** 394 (2002)]
28. Maksimov E G, Dolgov O V, Kulić M L *Phys. Rev. B* **72** 212505 (2005)
29. Phillips J C *Phys. Rev. B* **71** 184505 (2005)
30. Lee J et al. *Nature* **442** 546 (2006)
31. Newns D M, Tsuei C C *Nature Phys.* **3** 184 (2007)
32. Gedik N et al. *Science* **316** 425 (2007)
33. Radovic Z, Bozovic N, Bozovic I *Phys. Rev. B* **77** 092508 (2008)
34. Kirillov D, Bozovic I, Char K, Kapitulnik A *J. Appl. Phys.* **66** 977 (1989)
35. Reedyk M, Timusk T *Phys. Rev. Lett.* **69** 2705 (1992)
36. Bozovic I et al. *Phys. Rev. Lett.* **73** 1436 (1994)
37. Uchida S et al. *Phys. Rev. B* **43** 7942 (1991)
38. Holstein T *Ann. Phys.* (New York) **8** 325 (1959)
39. Holstein T *Ann. Phys.* (New York) **8** 343 (1959)
40. Bozovic I *Phys. Rev. B* **48** 876 (1993)

PACS numbers: **74.62. – c**, **74.40. – b**, **74.78. – w**

DOI: 10.1070/PU2008v051n02ABEH006467
DOI: 10.3367/UFNr.0178.200802h.0190

Structural design of superconductors based on complex copper oxides

E V Antipov, A M Abakumov

1. Introduction

The design of new materials with important physical properties is one of the challenging problems of modern science. A variety of approaches are being developed in order to overcome labor-consuming exhaustive search of chemical compositions and synthesis conditions and to optimize the solution to this problem. Structural design is one of the most effective methods. This method involves an analysis of chemical composition – structure – property relations for a certain class of materials, possible structure types for a set of chemical elements that can be used to form the required crystal structure, the coordination environment of atoms in the structure, and the character of bonds between various atomic groups. Researchers from the Inorganic Crystal Chemistry Laboratory of the Chemical Department of Moscow State University used a structural design to search for new high-temperature superconductors based on complex copper oxides. In this report, we do not consider the crystal chemistry of high-temperature superconductors in detail. The main purpose is to describe the crystal chemistry principles of designing new superconductors that were used to fabricate new members of this unique family of materials and to predict ways to optimize their properties.

2. Structure and strategy of searching for new high-temperature superconductors based on complex copper oxides

Studying the relation between the composition, structure, and properties of numerous copper-containing high-temperature superconducting (HTSC) oxides has allowed formulating the following structural and chemical criteria required for the appearance of these properties:

(i) a layered structure in which (CuO_2) layers represent an infinite network of copper – oxygen CuO_4 squares connected by their vertices (Fig. 1);

(ii) optimum Cu – O interatomic distances in the layer plane (1.90 – 1.97 Å) to provide the overlapping of the $3d_{x^2-y^2}$ copper orbitals and the $2p_{x,y}$ oxygen orbitals with the formation of delocalized states in the σ^* band; and

(iii) an optimum carrier concentration in the (CuO_2) layers that corresponds to the formal copper oxidation state +2.05 to +2.25 for hole-doped superconductors and +1.8 to +1.9 for electron-doped superconductors.

Copper atoms can also be bound to oxygen atoms located in neighboring layers. However, these bonds are significantly longer and exceed 2.2 Å. Copper cations in the structures of superconductors have different chemical bonds with oxygen atoms: strong (planar) bonds in the (CuO_2) layer plane and much weaker (axial) bonds in the normal direction. The structures of the superconductors based on complex copper oxides are layered, and the framework structures of these oxides do not have superconducting properties.

Due to its negative charge, the (CuO_2) layer should be located between positive-charged or neutral cation – anion layers. Obviously, the most convenient layers are (AO) or ($A'\square$) (where $\square$ is an anion vacancy) layers. Figure 2 shows the (CuO_2) layer located between such layers in the two simplest structures, perovskite ABO_3 and $CaCuO_2$ (tetragonal anion-deficient perovskite structure). The structure (i.e., atomic positions and geometric characteristics) of this layer is optimum for the perovskite structure ABO_3, which contains layers of two types, (AO) and (BO_2), alternating along a fourfold axis. Therefore, all superconducting complex copper oxides have structures that are derivative of perovskite or contain a perovskite-like fragment as one of the structural blocks.

A complex oxide with a perovskite structure can be synthesized if the electric neutrality criterion is satisfied and the cation – anion distances correspond to the Goldschmidt

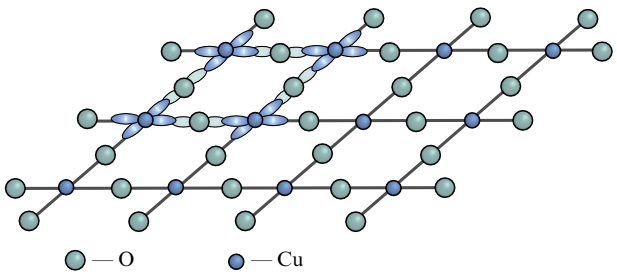

Figure 1. Structure of the copper – oxygen (CuO_2) layer.

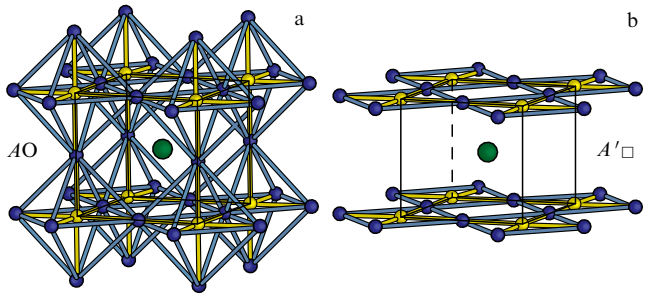

Figure 2. Structures of ABO_3 perovskite (a) and $CaCuO_2$ (b), in which (CuO_2) layers alternates with (AO) or ($A'\square$) layers.

criterion $d_{A-O} \approx \sqrt{2} d_{B-O}$. When Cu^{2+} is chosen as the B cation, electric neutrality is the main problem. The copper cations in the (CuO_2) layers have the formal oxidation state close to +2; therefore, the formal charge of this layer should be close to −2, and the charge of the (AO) layer should correspondingly be equal to +2. This makes it difficult to choose the A-type cation, since metals with the formal charge +4 have very small radii, coordination numbers, and interatomic distances to oxygen. These contradictions can be resolved by synthesizing compounds with anion-deficient perovskite-like ABO_{3-x} structures ($0 < x \leqslant 1$, e.g., $CaCuO_2$ or $YBa_2Cu_3O_{7-\delta}$) or compounds with intergrowth structures, which represent most well-known superconducting complex copper oxides.

Despite the variety of compositions of superconducting phases with intergrowth structures, they can be described by the general formula $B_m A_2 A'_{n-1} Cu_n O_{2n+2+x}$, which can be represented as the sequence of layers

$$(AO)\,(BO_x)_m(AO)\,(CuO_2)\left[(A'\square)(CuO_2)\right]_{n-1}$$
$$\times\,(AO)(BO_x)_m(AO)\,,$$

where $0 \leqslant x \leqslant 1$, $m = 0, 1, 2$, $n = 1, 2, 3, \ldots$, A and A' are the respective cations of alkaline-earth or rare-earth metals and B is the smaller cation (e.g., Hg^{2+}, Tl^{3+}, Bi^{3+}). These layers are formally joined to yield blocks of the perovskite, fluorite, or sodium chloride type, since the arrangement of cations and anions in these fragments corresponds to their arrangement in these simplest inorganic structures. For the fluorite block (R_2O_2), the sequence of three $(R)\,O_2(R)$ layers (where R is a tri- or tetravalent rare-earth element) appears instead of the ($A'\square$) layer. Superconducting (CuO_2) layers are located in perovskite blocks, and their number per unit cell varies from 1 to n (usually, n does not exceed 5–7). If $n \geqslant 2$, oxygen-free ($A'\square$) layers or a fluorite block at $n = 2$ are placed between these layers. The remaining dielectric blocks ensure structure stability; in particular, they compensate for the negative charge of the (CuO_2) layer. These fragments have a positive formal charge, which can be varied by heterovalent cation (anion) substitution or a change in the oxygen content; as a result, the hole concentration that is optimal for superconductivity can be achieved in the conduction band. Figure 3 shows a schematic diagram for the formation of an intergrowth structure, in which the perovskite block alternates with the NaCl and fluorite blocks.

The lattice parameters of the cubic unit cells of a number of oxides with NaCl- and CaF_2-type structures fall in the range 5.2–5.7 Å. The cation–cation distances in these structures are close to the corresponding distances in perovskite-type structures, in which the parameter a is

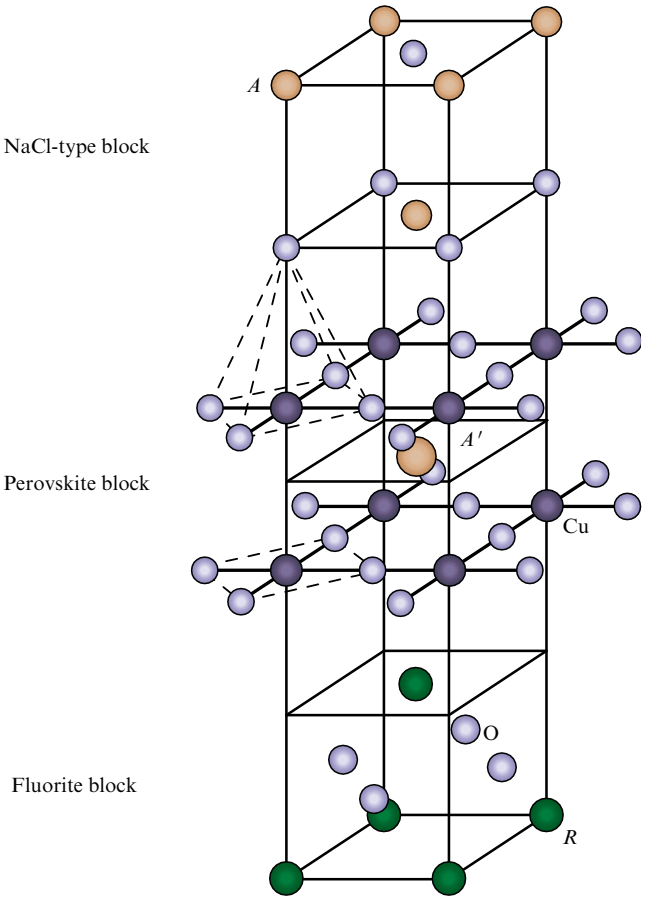

Figure 3. Schematic diagram for the formation of an intergrowth structure with alternating structural blocks of the NaCl, perovskite, and fluorite types.

usually 3.7–4.1 Å ($a_{NaCl} \approx a_{CaF_2} \approx \sqrt{2} a_{per}$). The face-centered cubic unit cells of the NaCl and fluorite types can be transformed into body-centered tetragonal cells with parameters a close to a_{per}. It is important that the cation motifs in the perovskite unit cell and the transformed fluorite and NaCl unit cells be the same and that the oxygen atom positions be different.

The layered character of the structures of all well-known copper HTSCs agrees with Ginzburg's "quasi-two-dimensional model," in which a planar conductor [in our case, copper-containing (CuO_2) layers] touches an insulator [blocks of the fluorite or sodium chloride type or ($AO/(A'\square)$ layers], e.g., a dielectric film. The development of this concept leads to the alternation of thin conducting and dielectric layers as in a 'sandwich' [1].

Structures with such layer sequences are stable only if the interatomic distances in any layer match with those in the upper and lower neighboring layers in the (ab) plane. A mismatch causes strong distortions in the (CuO_2) layers, which results in the degradation of superconducting properties down to the suppression of superconductivity. In the structures of Bi-containing $Bi_2Sr_2Ca_{n-1}Cu_nO_{2n+4+\delta}$ superconductors, the in-plane Cu–O distances fall in the range 1.9–1.95 Å; in this case, the Sr–O and Bi–O interatomic distances should be 2.7–2.75 Å, which is typical of the strontium cation and too large for the bismuth cation. Cooperative atomic displacements in the ($BiO_{1+\delta/2}$) layers eventually lead to the formation of the interatomic distances

and coordination numbers typical of this cation. The sequence of such atomic displacements (incommensurate modulations) becomes possible due to the introduction of an additional oxygen atom (δ) into approximately every fifth cell. Otherwise, the displacements of Bi and O atoms would result in the location of like-charged ions in two successive (BiO) layers immediately above each other. The cooperative displacements and the introduction of an additional oxygen atom restore the matching of alternating layers in Bi – HTSC structures but introduce distortions in these layers, including the (CuO_2) layer. In a strongly distorted $Bi_{2+x}Sr_{2-x}CuO_{6+\delta}$ structure, T_c does not exceed 20 K in spite of the hole concentration in the conduction band that is optimal for superconductors of this type. The superconducting transition temperature increases to 86 and 108 K for the second and third members of the Bi-containing homologous series, which have much smaller distortions in the (CuO_2) layers. However, the possibilities of a further increase in T_c in the family of $Bi_2Sr_2Ca_{n-1}Cu_nO_{2n+4+\delta}$ superconductors due to an increase in the number of (CuO_2) layers in the perovskite block are exhausted, since the amount δ of hyperstoichiometric oxygen bound to bismuth cations by strong bonds cannot vary over a wide range and is similar for all compounds in the family.

Varying the cation composition of the blocks and the formal degree of copper oxidation states (which is accompanied by a change in the Cu – O distances) allows changing the block sizes and producing the required compound via a proper synthesis method. To predict new intergrowth structures, we must take into account the crystal-chemistry specific features of cations (the ionic radius, coordination number, character of the chemical bond with oxygen), the chemical compatibility of ions (the simultaneous absence of strong oxidizers and reducers), and the electric neutrality of the unit cell. The choice of the synthesis method should be dictated by the chemical features of the initial substances and the required degrees of oxidation of individual components in the final structure.

An important crystal-chemistry criterion for a high-T_c superconductor is the absence of strong local distortions in the (CuO_2) layer, which can be induced by a statistical joint location of different cations (e.g., di- and trivalent cations) in the same crystallographic position in neighboring layers. The difference in the crystal-chemistry properties of these cations leads to the formation of different coordination polyhedra with oxygen atoms, including oxygen atoms bound to copper atoms, which causes local distortions in the (CuO_2) layer. As these distortions increase, T_c decreases to the complete suppression of superconductivity.

Figure 4 shows the electron-density distribution of the oxygen atom in the axial position with respect to the copper cation from the (CuO_2) layer in the structure of $Nd_{1.7}Ba_{1.3}Cu_3O_{7.15}$ [2]. The electron density is seen to shift from the fourfold axis, which is caused by the joint location of barium and neodymium cations at the same crystallographic position. As a result of this shift, the Ba and Nd cations acquire their intrinsic coordination environments, which is accompanied by the appearance of various Cu – O axial bonds and strains in the (CuO_2) layer.

We note that the standard structural examination by neutron or X-ray diffraction can hardly reveal such distortions, since the refinement of atomic parameters only results in the enhanced thermal parameters of atoms, which reflect not a dynamic but a static character of displacements. To adequately describe the atomic arrangement, we have to use precise data on perfect single crystals, obtaining which involves significant experimental difficulties. Attfield et al. [3] proposed using the disorder parameter σ^2 that characterizes

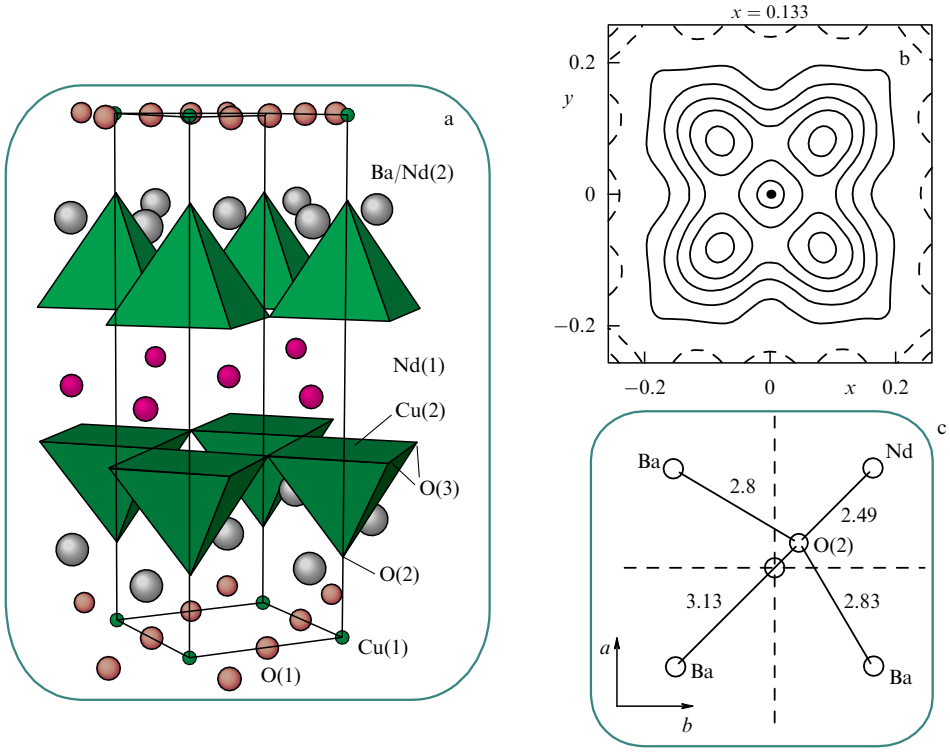

Figure 4. (a) Crystal structure of $Nd_{1.7}Ba_{1.3}Cu_3O_{7.15}$, (b) electron density map of the oxygen atom O(2), and (c) Nd – O(2) and Ba – O(2) interatomic distances.

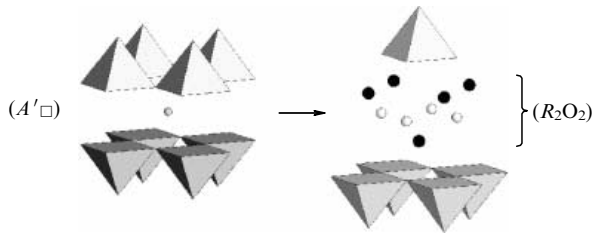

Figure 5. Schematic diagram of the substitution of the fluorite block (R_2O_2) for the $(A'\square)$ layer in the structures of layered copper oxides.

the difference in the sizes of the cations statistically located at the same position, in order to estimate the linear decrease in T_c as this parameter increases.

This reason is thought to be the main factor that results in the low values of T_c or the absence of superconductivity in all intergrowth structures that contain fluorite fragments and tetravalent cations (Ce or Th) apart from trivalent rare-earth cations. Intergrowth structures with a fluorite block can be formally described as the result of a 'substitution' of the fluorite block (R_2O_2) for an $(A'\square)$ layer located between two (CuO_2) layers in a prototype structure. This substitution results from the closeness of the fluorite and perovskite block sizes in the (*ab*) plane and from the charge balance (Fig. 5). Table 1 gives the maximum values of T_c for various fluorite-block-containing superconductors and their prototype structures. The superconducting transition temperatures of the fluorite-block-containing compounds are well below those of the prototype structures. This can be due to the statistical distribution of different cations in the layers next to (CuO_2) layers, which induces a structural disorder and local distortions in these layers.

Table 1. T_c of complex copper oxides with fluorite blocks and the prototype structures.

'Fluorite' phase	T_c	Prototype structure	T_c
$La_{0.9}Sm_{0.9}Sr_{0.2}CuO_{3.97}$	27 K [4]	$La_{1.6}Sr_{0.4}CaCu_2O_6$	60 K [5]
$Pb_2Sr_2Eu_{1.33}Ce_{0.67}Cu_3O_{10}$	24 K [6]	$Pb_2Sr_2Y_{0.6}Ca_{0.4}Cu_3O_8$	70 K [7]
$Bi_2Sr_2Eu_{1.7}Ce_{0.3}Cu_2O_{10+\delta}$	28 K [8]	$Bi_2Sr_2CaCu_2O_{8+\delta}$	86 K [9]
$Eu_2Ba_{1.33}Ce_{0.67}Cu_3O_{8+\delta}$	40 K [10]	$YBa_2Cu_3O_{7-\delta}$	93 K [11]

3. Mercury-containing superconducting complex copper oxides $HgBa_2Ca_n$

The structures of most Cu-containing superconductors have a fragment consisting of three alternating layers, $(CuO_2)(AO)(BO)$ (Fig. 3, NaCl-type block). Structures with such layer sequences are stable only when the interatomic distances in any layer match those in the upper and lower neighboring layers, and the correspondence between the (CuO_2) and (AO) layers is most important. From the standpoint of a geometrical criterion, Ba^{2+}, Sr^{2+}, and La^{3+} are optimum cations for position *A*. The use of alkaline-earth metal cations of proper sizes in this position along with other structural fragments cannot compensate for the excess negative charge of the (CuO_2) layer in oxide structures. For T_c to be high in complex copper oxides, the cation positions in the layers next to (CuO_2) should be occupied by cations of the same type. Otherwise, the difference in the crystal-chemistry properties of the cations placed at the same position causes local distortions in the structure, which decreases T_c and eventually suppresses superconductivity [3].

Since the crystal-chemistry properties of *A*-type cations strongly affect the structure of the (CuO_2) layer and, correspondingly, the conducting properties of compounds, we assumed that compounds with the cations of divalent mercury in the *B*-type position could have the optimum structure. In oxide phases, these cations are characterized by a dumbbell coordination, which is realized, e.g., in $MHgO_2$ (M = Ca, Sr, Ba) structures. For such a coordination to form near Hg^{2+} cations, the structure of a layered oxide should have oxygen atoms only in neighboring layers, and their presence in the layer with the mercury cations is not necessary. The absence of steric difficulties and the weak chemical bond with neighboring cations allow changing the occupation of the anion position with oxygen atoms and varying the hole concentration in the conduction band. We also note that Hg^{2+} cations have the optimum formal charge for achieving the electric neutrality of the structure. In these structures, there should be no mismatch of the (AO), (HgO_δ), and (CuO_2) layers because the Hg–O bond in the (HgO_δ) layer should be too weak to substantially affect the matching with other structural fragments and the superconducting properties of layered copper oxides with this structural block.

Cystal-chemistry has allowed predicting a new family of superconductors $HgBa_2Ca_{n-1}Cu_nO_{2n+2+\delta}$. In Section 4, we briefly discuss their crystal structures and superconducting properties. Detailed information is given in review [12].

4. Crystal structures of $HgBa_2Ca_{n-1}Cu_nO_{2n+2+\delta}$

The structures of the first three members of the family are shown in Fig. 6. The structures of $HgBa_2Ca_{n-1}Cu_nO_{2n+2+\delta}$ can be schematically represented as the following sequence of layers alternating along the unit-cell *c* axis:

$$(HgO_\delta)(BaO)(CuO_2)\{(Ca)(CuO_2)\}_{n-1}(BaO)(HgO_\delta)\,.$$

All compounds have tetragonal primitive cells with similar parameters *a*, and the parameter *c* increases with the perovskite fragment thickness in accordance with the formula $c \approx 9.5 + 3.2 \times (n-1)$[Å].

The structures of $HgBa_2Ca_{n-1}Cu_nO_{2n+2+\delta}$ are very close to the corresponding structures of the compounds of the homologous series $TlBa_2Ca_{n-1}Cu_nO_{2n+2+\delta}$. The main difference is in the number of oxygen atoms in layers with Hg or Tl

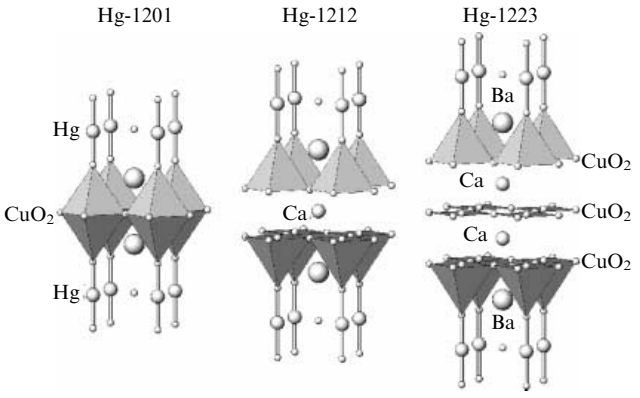

Figure 6. Crystal structures of $HgBa_2Ca_{n-1}Cu_nO_{2n+2+\delta}$ with n = 1, 2, and 3.

atoms. In the structures of the Tl-containing superconductors, the filling of the oxygen position δ insignificantly differs from unity irrespective of the number of (CuO_2) layers in the structures, since these oxygen atoms are required for the creation of the characteristic coordination of Tl^{3+} ions. In contrast, in the structures of $HgBa_2Ca_{n-1}Cu_nO_{2n+2+\delta}$, the content of weakly bound overstoichiometric oxygen in the Hg^{2+}-containing layer can vary within very wide limits by heat treatment at various temperatures and partial oxygen pressures. Overstoichiometric oxygen strongly affects the copper oxidation state in (CuO_2) layers and the superconducting transition temperature. For members of the homologous series $HgBa_2Ca_{n-1}Cu_nO_{2n+2+\delta}$, the formal copper oxidation state can be calculated by the formula $V_{Cu} = 2(n+\delta)/n$.

In the structures of this family, the NaCl-type block has the same structure in all compounds and consists of the three alternating layers (BaO), (HgO_δ), and (BaO). On the whole, δ increases with an increase in n; however, the δ ranges of various homologues can overlap. For example, the values of δ obtained by neutron diffraction are 0.06 – 0.23 for Hg-1201 [13, 14] and 0.08 – 0.35 for Hg-1212 [15 – 17]. The Hg^{2+} cations have a specific dumbbell surrounding of the nearest oxygen atoms from (BaO) layers with $d(Hg-O) \approx 1.95$ Å. Overstoichiometric oxygen atoms from the (HgO_δ) layer are far from mercury atoms ($d(Hg-O) \approx 2.7-2.76$ Å) and are not involved in the formation of a strong chemical bond with these cations.

As the perovskite-fragment thickness increases, the coordination of the copper atoms in (CuO_2) layers changes from an octahedral coordination in the structure of $HgBa_2CuO_{4+\delta}$ to a tetragonal – pyramidal coordination in $HgBa_2CaCu_2O_{6+\delta}$ and then to a square or tetragonal – pyramidal coordination in $HgBa_2Ca_2Cu_3O_{8+\delta}$ and the structures of the higher homologues. The octahedra and tetragonal pyramids are strongly elongated along the c-axis because of the Jahn – Teller distortion. Table 2 gives the Cu – O and Ba – O distances in the structures with $n = 1-3$.

The specific feature of the structure of Hg-containing superconductors is a very long Cu – O distance to the axial oxygen atom in the copper polyhedra, which vary in the range 2.75 – 2.8 Å for various members of the series; as a result, the interaction between these atoms is very weak. This distance is much longer than the corresponding distances in the structures of other copper-containing superconductors. For example, the Cu – O distance in $YBa_2Cu_3O_7$ ($T_c = 92$ K) is 2.32 Å. Another peculiar feature is the absence of significant atomic displacements in layers due to the absence of mismatch. Introduced oxygen atoms do not cause a superstructure or orthorhombic distortions, since they are located at the center of a square formed by mercury atoms. Therefore, the structure of the (CuO_2) layers in Hg-containing superconductors is closest to the ideal structure, as compared to the structures of the well-known superconducting complex copper oxides. The (CuO_2) layers in Hg-1212 and Hg-1223 are almost planar despite the asymmetric tetragonal – pyramidal copper coordination. This ideal structure is likely to be the main cause of superconductivity in these compounds at temperatures that are maximal among the temperatures of all well-known superconductors.

In $HgBa_2Ca_{n-1}Cu_nO_{2n+2+\delta}$, the in-plane Cu – O distances decrease with increasing δ (due to the oxidation of copper atoms) or with increasing the perovskite-fragment thickness. In the latter case, it is interesting to analyze the relation between the changes in the various interatomic distances when moving to structures with a large number of (CuO_2) layers. For the same of copper oxidation state to be achieved in these structures, the amount of hyperstoichiometric oxygen introduced into the Hg-containing layer should increase as n increases. As a result, the fraction of barium atoms that move toward an additional anion increases, which is accompanied by a decrease in the $Ba-O_{Hg}$ distances and an increase in the $Ba–O_{Cu}$ distances between Ba^{2+} cations and oxygen atoms from the (CuO_2) layer (Fig. 7, Table 2). Thus, the interaction between Ba atoms and these oxygen atoms weakens, which is compensated by a decrease in the in-plane Cu – O distance. Therefore, the sequential increase in

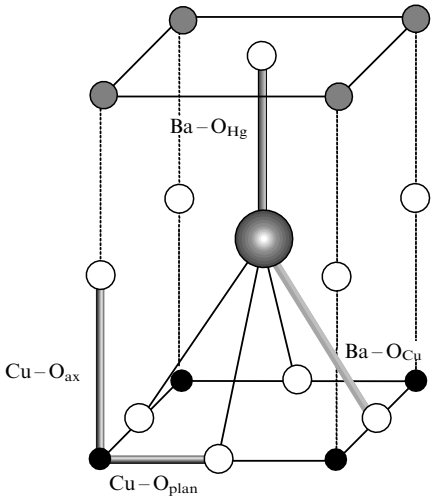

Figure 7. Some interatomic distances in $HgBa_2Ca_{n-1}Cu_nO_{2n+2+\delta}$.

Table 2. Some interatomic distances [Å] in $HgBa_2Ca_{n-1}Cu_nO_{2n+2+\delta}$ ($n = 1-3$).

Compound	δ	$Cu-O_{plan}$	$Cu-O_{ax}$	$Ba-O_{Hg}$	$Ba-O_{Cu}$
Hg-1201	0.06	1.9432	2.803	2.866	2.726
	0.12	1.9426	2.787	2.841	2.733
	0.19	1.9398	2.771	2.834	2.734
	0.23	1.9365	2.750	2.787	2.751
Hg-1212	0.08	1.9320	2.824	2.848	2.733
	0.22	1.9290	2.799	2.807	2.758
	0.28	1.9272	2.798	2.773	2.773
	0.35	1.9263	2.787	2.749	2.778
Hg-1223*	0.41	1.9252	2.751	2.55, 2.94	2.92, 2.63

* Data for two positions of Ba atoms.

the perovskite-fragment thickness in the structures of $HgBa_2Ca_{n-1}Cu_nO_{2n+2+\delta}$ induced by the introduction of an additional $CaCuO_2$ block compresses the in-plane interatomic distances in structures of the higher homologues and can be represented as an anisotropic 'chemical' compression. The in-plane Cu – O interaction strongly affects the critical superconducting transition temperature (see Section 5).

The sequential increase in the perovskite-fragment thickness does not cause substantial changes in the structures of the highest homologues. It is difficult to study the structures of these compounds because of impurities and high stacking-fault concentrations. As n increases, the concentration of these defects, in which the sequences of layers correspond to other members of the family, increases [18].

5. Superconducting properties of $HgBa_2Ca_{n-1}Cu_nO_{2n+2+\delta}$

The superconducting transition temperature of the $HgBa_2Ca_{n-1}Cu_nO_{2n+2+\delta}$ phases depends strongly on two parameters, the oxygen content δ and the number n of (CuO_2) layers in their structures. It is interesting that the dependences of these temperatures have a dome-like shape in both cases [19 – 21].

Figure 8 shows the dependence of T_c on n. The values of T_c correspond to the maximum values obtained for each superconductor. The superconducting transition temperature is seen to increase from the first member of the homologous series (97 K) to the second (127 K) and third (135 K) member, and then to decrease for the fourth (127 K), fifth (110 K, and sixth (107 K) members of this series. One of the possible causes of the decrease in T_c in the higher homologues can be the distortion of the outer (CuO_2) layers with increasing n because of a decrease in the $Cu-O_{ax}$ distance. The enhancement of the interaction between these atoms shifts copper atoms from the plane toward the axial oxygen, which leads to a distortion of the O – Cu – O bond angle and a loss of planarity of these (CuO_2) layers.

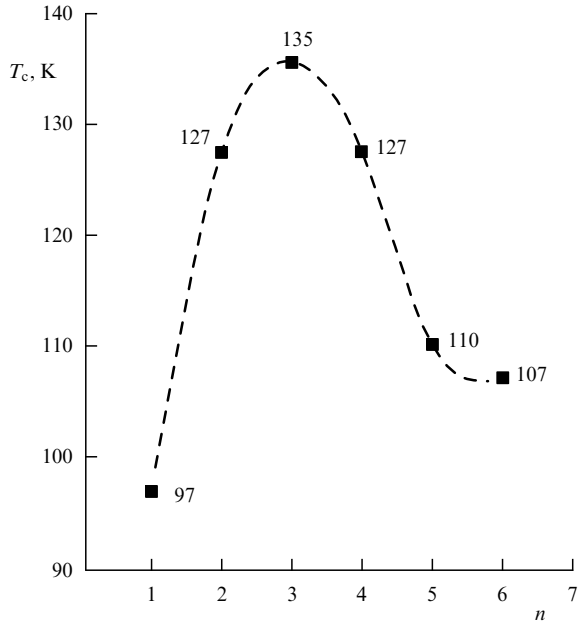

Figure 8. T_c vs. the number n of (CuO_2) layers for the compound $HgBa_2Ca_{n-1}Cu_nO_{2n+2+\delta}$.

Generally, the superconducting transition temperature of a complex superconducting copper oxide depends on the hole concentration in the conduction band (or on the formal degree of copper oxidation). The optimum degree of oxidation for hole-doped superconductors ranges from +2.10 to +2.20, where the compounds typically exhibit maximum values of T_c. Outside this range, T_c decreases. Thus, the dependence of the superconducting transition temperature on the formal copper oxidation state should have a dome-like character. This rule holds in the case of only one type of oxidized elements [i.e., copper atoms in the (CuO_2) layer] in the structure of a superconductor.

If there are several types of copper atoms or another oxidizable element, this dependence is much more complex, since charges can be redistributed between different structural fragments. T_c is also strongly affected by the factors that determine the structure of the (CuO_2) layers.

It was shown above that the structures of the $HgBa_2Ca_{n-1}Cu_nO_{2n+2+\delta}$ compounds are optimal for the appearance of superconductivity, since they have no distortions induced by a mismatch of interatomic distances and a nonuniform cation distribution in neighboring layers. Moreover, the structures of the first members of the homologous series ($HgBa_2CuO_{4+\delta}$ and $HgBa_2CaCu_2O_{6+\delta}$) only have one type of copper atom. Therefore, the dependence of T_c on the formal degree of copper oxidation, which is changed by varying δ, should have a dome-like character for these compounds, which is supported experimentally. Superconductivity in $HgBa_2CuO_{4+\delta}$ can be suppressed as the index δ strongly increases. The nonsuperconducting overoxidized compound Hg-1201 was synthesized at a high pressure. For this compound, $V_{Cu} = +2.28$ corresponds to the V_{Cu} range outside which superconductivity is suppressed [14]; such ranges were established previously for other superconducting copper oxides.

For members of the homologous series with $n \geqslant 2$, it is difficult to use iodometric titration to determine V_{Cu} because of the presence of impurity phases. The Cu – O distance in the (CuO_2) layer depends on the formal copper oxidation state, which is changed by varying δ. Since this layer is planar, the unit-cell parameter a of the Hg-containing superconductors is approximately twice the Cu – O distance. Therefore, a change in the parameter a after various heat treatments indicates the character of the change in δ. Figure 9 shows the $T_c(a)$ dependences for five members of the family that also have a dome-like character. It is interesting that the maximum values of T_c increase in the Hg-1201 – Hg-1212 – Hg-1223 series as the parameter a [hence, the $Cu-O_{plan}$ distance (see Table 2)] decreases. The cause of this increase was discussed in Section 4. Thus, the sequential increase in the perovskite-fragment thickness in this series of compounds can be formally considered a structural modification that causes anisotropic compression of the in-plane interatomic distances, which can lead to an increase in T_c.

Chu et al. [22] were the first to detect a substantial increase in T_c in $HgBa_2Ca_2Cu_3O_{8+\delta}$ at ultrahigh pressures. The superconducting transition temperature of this compound increases sharply with the applied pressure and reaches 164 K at the pressure about 31 GPa [23, 24]. The pressure-induced increase in the superconducting transition temperature in Cu-containing superconductors, which exhibit hole conductivity in the normal state, is a well-known phenomenon. Nevertheless, the specific feature of the experiments performed on Hg-1223 and other compounds of this family lies in achieving

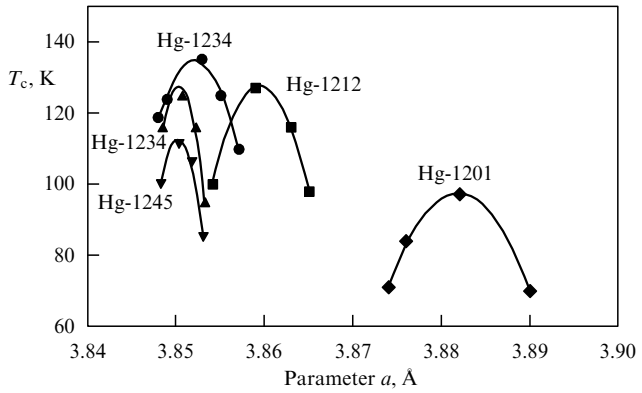

Figure 9. T_c vs. parameter a for $HgBa_2Ca_{n-1}Cu_nO_{2n+2+\delta}$ compounds.

record values of T_c, which are well above those reached previously. These results demonstrate that superconductivity with $T_c = 150-160$ K can exist at atmospheric pressure in structures where the Cu – O distances are identical to those realized in $HgBa_2Ca_{n-1}Cu_nO_{2n+2+\delta}$ at an applied pressure.

Using neutron diffraction under pressure, the authors of [25–29] revealed the main trends in the variation of the interatomic distances in these superconductors. As the pressure increases, the Hg – O bond length remains virtually the same because of the strongly covalent character of this bond. The compression of the structures along the c-axis is caused by a significant decrease in the axial Cu – O distance. An isotropic applied pressure also decreases the in-plane Cu – O distance, but to a lesser extent.

Interesting conjectures can be made regarding the different characters of the dependences of the superconducting transition temperature on the applied isotropic pressure and the anisotropic chemical compression of the in-plane Cu – O distances, which is induced by an increase in the perovskite-fragment thickness in the Hg-1201 – Hg-1212 – Hg-1223 series. In this series, the axial Cu – O distances are virtually unchanged (see Table 2), which suggests the strongest effect of the in-plane distance on T_c. The value of $dT_c/d(Cu-O_{plan})$ calculated from the structural data for these compounds with the maximum values of T_c exceeds -1000 K Å^{-1} for this series. However, for isotropic applied pressure, this value is substantially lower (~ -160 K Å^{-1}).

6. Fluoro-substituted derivatives of superconducting mercury-containing cuprates

Important conclusions concerning the doping mechanism and the effect of the in-plane and axial Cu – O distances on T_c in mercury cuprates can be drawn by comparing the characteristics (the anion content, the formal copper oxidation state, the structural parameters, the superconducting transition temperature) of samples in which the optimum level of doping was achieved by the introduction of additional oxygen or fluorine. Oxygen and fluorine are similar from the crystal-chemistry standpoint and have high electric negativity, and their anions have similar ionic radii ($r_{F^-} = 1.29$ Å and $r_{O^{2-}} = 1.35$ Å for coordination number 2). Moreover, many oxide compounds exhibit structural analogues between fluorides and oxofluorides (CaO and NaF, LaOF and CaF_2, La_2CuO_4 and K_2CuF_4, etc.). Therefore, when fluorine is introduced into complex layered copper oxides, related oxofluorides can form. The formal charges of O^{2-} and F^- are different, and, according to a simple ionic model of hole formation in a conducting (CuO_2) layer, the amount of fluorine anions required for a certain doping level is twice that of oxygen anions.

The fluorination of the Hg-1201 phase $HgBa_2CuO_{4.01}$ with $T_c = 61$ K by xenon difluoride XeF_2 leads to an increase in the superconducting transition temperature to the maximal value for this compound ($T_c = 97$ K), the subsequent decrease in T_c, and, eventually, the suppression of superconductivity, presumably because of too high a copper oxidation state (overoxidation) [30]. According to neutron powder diffraction data, the anion content in the Hg-containing layer is $\delta = 0.24(2)$ for an optimally doped sample with $T_c = 97$ K and $\delta = 0.32(2)$ for an overoxidized sample with $T_c = 80$ K. These values are well above the occupations found for oxidized Hg-1201 samples with close values of T_c ($\delta = 0.124(9)$ and 0.19(1), respectively) [13]. The dependences of T_c on the fluorine or oxygen content in the Hg-containing layer have a domelike shape; however, the curve for the fluorinated samples shifts toward higher values of δ (Fig. 10a). We can conclude that, like oxygen, fluorine oxidizes copper cations in (CuO_2) layers and that the amount of fluorine required for achieving certain values of T_c and a certain degree of doping is twice that of oxygen, which agrees with the difference in the formal charges O^{2-} and F^-. This finding supports the ionic model of doping in mercury cuprates: the number of holes created by one oxygen atom is twice that induced by one fluorine atom.

For both the fluorinated and oxidized samples, the dependences of T_c on the unit-cell parameter a (or, equivalently, on the $Cu-O_{plan}$ interatomic distance in the (CuO_2) layer plane) can be approximated by one parabolic curve with a maximum ($T_c = 97$ K) at $a = 3.882$ Å (Fig. 10b). Thus, the same superconducting transition temperatures can be achieved not only at the same level of doping but also at similar lengths of the in-plane Cu – O bonds; that is, both parameters control T_c in complex cuprates.

For a certain copper oxidation state, the $Cu-O_{plan}$ distance is virtually independent of the amount of overstoichiometric anions. In contrast, the $Cu-O_{ax}$ distance changes significantly as the degree of filling the anion position in an Hg-containing layer is varied. The dependence of this distance on δ (for oxygen or fluorine) is almost linear (Fig. 10c). An increase in the amount of hyperstoichiometric anions results in compression of the $Cu-O_{ax}$ bond, whose length in the fluorinated compounds is substantially smaller than that in the oxygen-containing compounds having similar values of T_c.

The cause of the decrease in the $Cu-O_{ax}$ distance consists in the extension of the Hg – O dumbbells induced by the increase in the coordination number of mercury atoms due to additional anions in the Hg-containing layer. As a result, an oxygen atom O_{ax} shifts from Hg to a Cu atom, which is accompanied by a noticeable decrease in the $Cu-O_{ax}$ distance, while the $Cu-O_{plan}$ distance and T_c remain virtually unchanged. This change in the interatomic distances can be considered a result of the anisotropic compression of the CuO_6 octahedra, which is equivalent to the effect of a pressure of about 2 GPa applied along the c-axis [29]. For the optimally oxygen-doped Hg-1201 phase, $dT_c/dP \approx 2$ K GPa^{-1} [31]; therefore, in a fluorinated sample with $\delta_F \approx \delta_{opt}$, the superconducting transition temperature should increase by ≈ 4 K. The absence of a difference in the values of T_c for the samples optimally doped by fluorine or oxygen indicates that the compression of the $Cu-O_{ax}$ bond

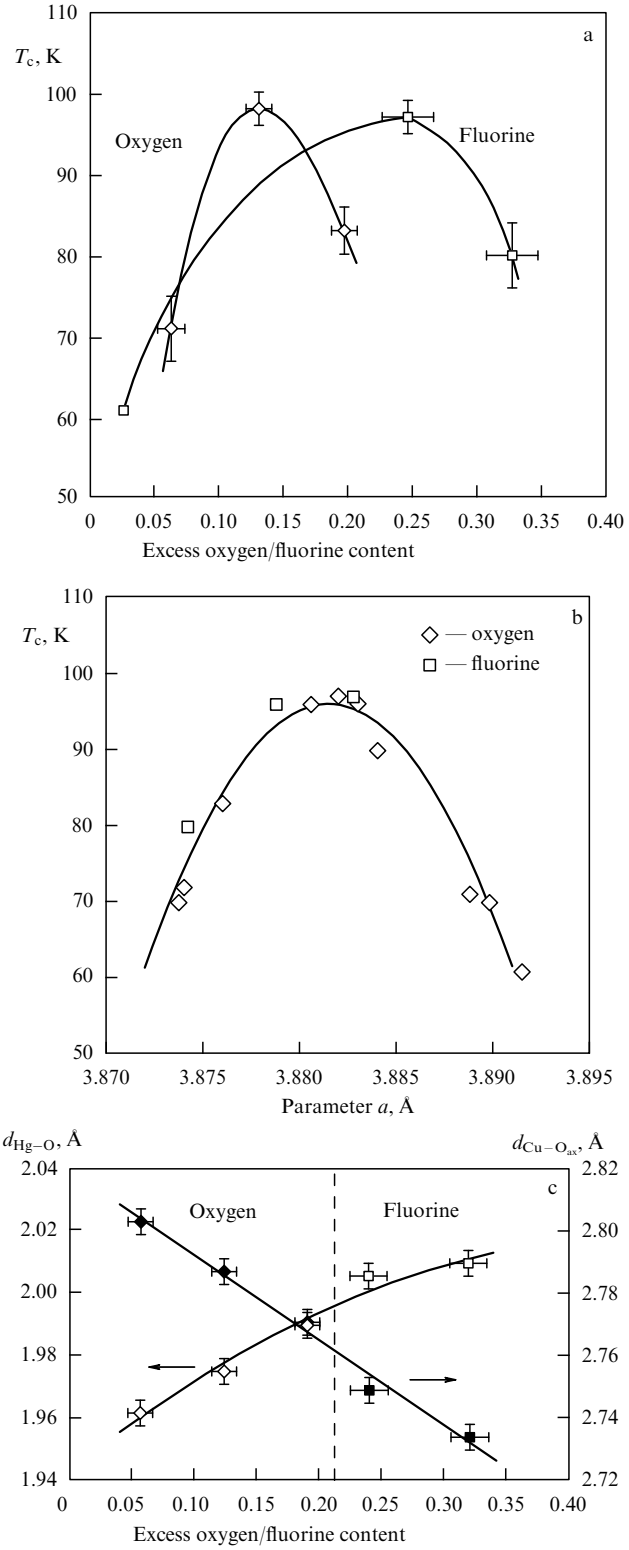

Figure 10. (a) Dependence of T_c on the excess oxygen or fluorine content for the Hg-1201 phase. (b) Dependence of T_c on unit-cell parameter a for Hg-1201 samples with various oxygen and fluorine contents. (c) Dependences of the $Cu-O_{ax}$ and Hg–O interatomic distances on the amount of oxygen or fluorine atoms in the mercury layer.

only weakly affects the increase in T_c in Hg-containing cuprates at an applied pressure and that the most probable cause of this phenomenon lies in a decrease in the $Cu-O_{plan}$ distances.

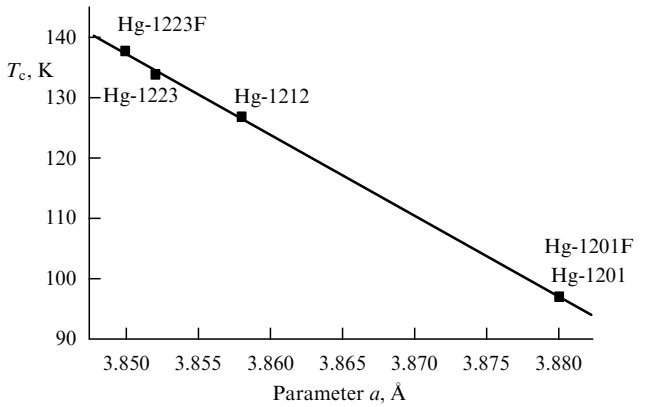

Figure 11. Maximum values of T_c vs. the unit-cell parameter a for oxidized and fluorinated Hg-containing cuprates.

This conclusion is also confirmed by the results of studying fluorinated $HgBa_2Ca_2Cu_3O_{8+\delta}$ (Hg-1223) samples. The initial Hg-1223 sample with $T_c = 100$ K exhibits an increase in T_c upon both fluorination and oxidation; however, T_c of the fluorinated sample is 4 K higher (138 K) than that of the oxidized sample (134 K) [32, 33]. It is interesting that this fluorinated sample has the highest T_c ($T_c = 166$ K at the pressure 23 GPa) among all superconductors [34]. The maximum values of T_c for the first three members of the homologous series of mercury-containing complex $HgBa_2Ca_{n-1}Cu_nO_{2n+2+\delta}$ cuprates and fluorinated Hg-1201 and Hg-1223 samples depend on the parameter a linearly, and we have $dT_c/da \approx -1350$ K Å^{-1} (Fig. 11) [33, 35]. We can state that T_c of these compounds depends on the compression of the (CuO_2) planes induced by the modification of the chemical composition. A similar value of dT_c/da was also detected upon the epitaxial compression of thin $La_{0.9}Sr_{0.1}CuO_4$ single-crystal films [36]. The value of dT_c/da observed upon the fluorination of Hg-1223 is almost an order of magnitude higher than the value induced by applied pressure ($dT_c/dP \approx 1.7$ K GPa$^{-1} \equiv dT_c/da \approx -160$ K Å^{-1}). This difference can result from a structural distortion of the (CuO_2) layers. In Hg-1201, these layers are planar by their symmetry, and, in Hg-1212, the $Cu-O_{plan}-Cu$ angle is close to 180° [17]. For Hg-1223, fluorination exerts a weak effect on the $Cu-O_{plan}-Cu$ angle: it is 178.4° for an oxidized sample [28] and 177.3° for a fluorinated sample [33]. A high applied pressure leads to folded (CuO_2) layers; for example, in Hg-1223, the $Cu-O_{plan}-Cu$ angle decreases to 175.0° at the pressure 2 GPa, which increases T_c to 138 K. The deviation of this valence angle from 180° is also an important parameter affecting T_c; for cuprates with $T_c > 100$ K, this deviation does not exceed 4°.

7. Fluoro-substituted derivatives of other families of superconducting cuprates

The specific feature of the structure of Hg-containing cuprates is that the Hg-containing layer has an anion position that can be partly occupied by oxygen or fluorine atoms, which results in various hole concentrations in the conduction band. A stable dumbbell-like coordination of the Hg^{2+} cations causes the absence of steric difficulties and a weak interaction between anions and mercury cations in this layer. Owing to the formation of a long and weak Hg–(O, F) bond in the layer plane, the introduction of anions into this layer does not lead to significant structural changes. How-

ever, the appearance of overstoichiometric anions in the structure of complex cuprates due to the introduction of fluorine or the substitution of two F^- anions for one O^{2-} anion can lead to structural transformations, which include changes in the coordination polyhedra, the interatomic distances, and the space symmetry up to complete rearrangement of the crystal structure. These transformations can be expected if fluorine anions form strong covalent or ionic bonds with neighboring cations. The fluorination of complex cuprates can be used for both producing new compounds with a structure required for the manifestation of superconducting properties and achieving the required carrier (electron or hole) concentration in the conduction band. The character of the change in the crystal structure is determined by the structure of the initial compound and the excess-anion content [37]:

(i) The replacement of oxygen atoms by the equivalent amount of fluorine atoms only causes insignificant changes in the unit-cell metric, which are related to the small difference in the ionic radii O^{2-} and F^- and to an increase in the in-plane Cu – O bond length due to the decreasing copper oxidation state.

(ii) The introduction of excess fluorine atoms and the completion of the coordination polyhedron of Cu^{2+} cations to an octahedron lead to a sharp increase in the axial Cu – O bond length, which is accompanied by an increase in the distances between the $(Cu(O, F)_2)$ and (AO) layers.

(iii) The occupation of vacant anion positions by fluorine atoms suppresses the structural distortions induced by the ordering of oxygen atoms and anion vacancies.

(iv) The location of fluorine atoms in interlayer voids results in a structure transformation of the crystal structure in order to decrease the forces of electrostatic repulsion between interlayer anions and anions in neighboring layers.

The perovskite-like anion-deficient structure of the $R Ba_2Cu_3O_{6+\delta}$ (R-123) phases is represented by the idealized sequence of layers

$$-Cu\square O_\delta - BaO - CuO_2 - R\square - CuO_2 - BaO - Cu\square O_\delta -$$

(where $\square$ stand for anion vacancies). The anion positions in the $(Cu\square O_\delta)$ layer (Cu1 layer) can be fully vacant at $\delta = 0$, which corresponds to the structure of the tetragonal strongly reduced R-123 phase (which is not a superconductor, $V_{Cu} = +1.67$). The Cu1 atoms are in the dumbbell coordination characteristic of the Cu^{1+} cations (Fig. 12a). At $\delta \approx 1$, oxygen atoms occupy half the vacant positions in the Cu1 layer in an ordered manner, completing the coordination environment to a square (Fig. 12b). Chains of the CuO_4 squares connected by common vertices are oriented along the b-axis, which results in an orthorhombic distortion of the structure. Compounds with $\delta \approx 1$ have a hole concentration that is near-optimal for this structure and exhibit the highest superconducting transition temperature ($T_c = 93 - 94$ K) among the compounds of this class.

In 1987, Kistenmacher used simple crystal-chemistry considerations and predicted the presence of complex oxofluoride $YBa_2Cu_3O_6F_2$ in which anion vacancies in the (Cu1) layer are fully occupied by fluorine atoms. The copper oxidation stare in this compound is $V_{Cu} = +2.33$, which corresponds to the formula $YBa_2Cu_3O_7$ (oxygen-doped Y-123). This oxofluoride should have a tetragonal symmetry due to the substitution of two-dimensional (CuF_2) layers for copper – oxygen chains and could exhibit superconducting properties [38]. The introduction of fluorine atoms into the structure of the reduced nonsuperconducting compound $YBa_2Cu_3O_{6.11}$ occurs in the vacant anion positions of the (Cu1) layer and is accompanied by the formation of distorted CuO_2F_4 octahedra [39, 40]. According to the proposed structural model, this is accompanied by an increase in the axial Cu – O distance from 1.85 Å in $YBa_2Cu_3O_{6.11}$ to 2.3 – 2.5 Å in the fluorinated compound with the idealized composition $YBa_2Cu_3O_6F_2$ (Fig. 12c). The fluorination of the reduced nonsuperconducting compound $YBa_2Cu_3O_{6.11}$ leads to an increase in the copper oxidation state to $V_{Cu} = +2.14$ and the appearance of superconductivity at the temperature 94 K with a large superconducting-phase volume ($\approx 25\%$).

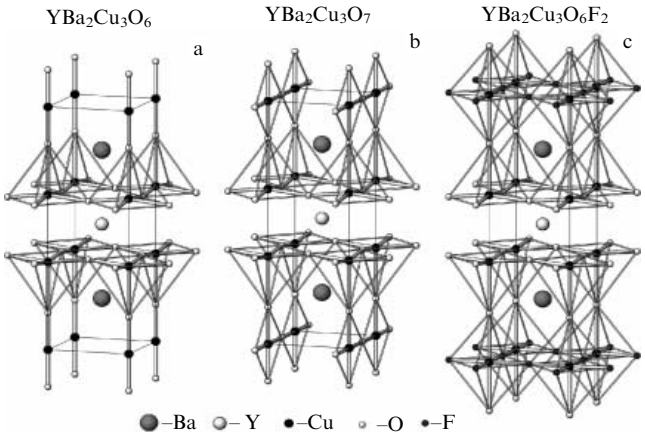

Figure 12. Crystal structures of $YBa_2Cu_3O_6$ (a), $YBa_2Cu_3O_7$ (b), and $YBa_2Cu_3O_6F_2$ (c).

One of the simplest copper oxofluorides with superconducting properties could be made from hypothetic perovskite-like $(La, Sr)CuO_2F$ solid solutions in which the required degree of copper oxidation is achieved via heterovalent substitution in the A sublattice. Such perovskites can be synthesized by fluorination of anion-deficient perovskites, such as $(La_{1-x}Sr_x)_8Cu_8O_{20-\delta}$ solid solutions, which have the framework structure of an anion-deficient perovskite without (CuO_2) planes and copper atoms with square, tetragonal – pyramidal, and octahedral environments (Fig. 13a). For a compound to be superconducting, fluorination should change the character of the oxygen distribution in the initial structure such that (CuO_2) planes form. When the compound $La_{6.5}Sr_{1.5}Cu_8O_{19.65}$ is fluorinated by xenon difluoride, the perovskite-like $La_{0.813}Sr_{0.187}Cu(O, F)_{3-\delta}$ phase forms with a tetragonally distorted unit cell with the parameters $a \approx c \approx a_{per}$ and $c > a$ (Fig. 13b) [41]. The anion positions in the equatorial environment of copper atoms are fully occupied and vacancies concentrate in the axial positions. The Jahn – Teller effect, which occurs because some copper atoms have an octahedral coordination, leads to an increase in the axial distances (2.026 Å) compared to the in-plane distances (1.896 Å) and a tetragonal distortion of the perovskite cell with $c > a$. The oxofluoride $La_{0.813}Sr_{0.187}Cu(O, F)_{3-\delta}$ is not a superconductor, which can be related to overoxidation, local distortions in (CuO_2) layers, and the possibility of partial substitution of fluorine for oxygen in the (CuO_2) layers (which transform them into $(Cu(O,F)_2$ layers). We believe that the use of other synthesis methods can result in successful synthesis of the oxofluoride $La_{0.85}Sr_{0.15}CuO_2F$ with an ordered oxygen and fluorine

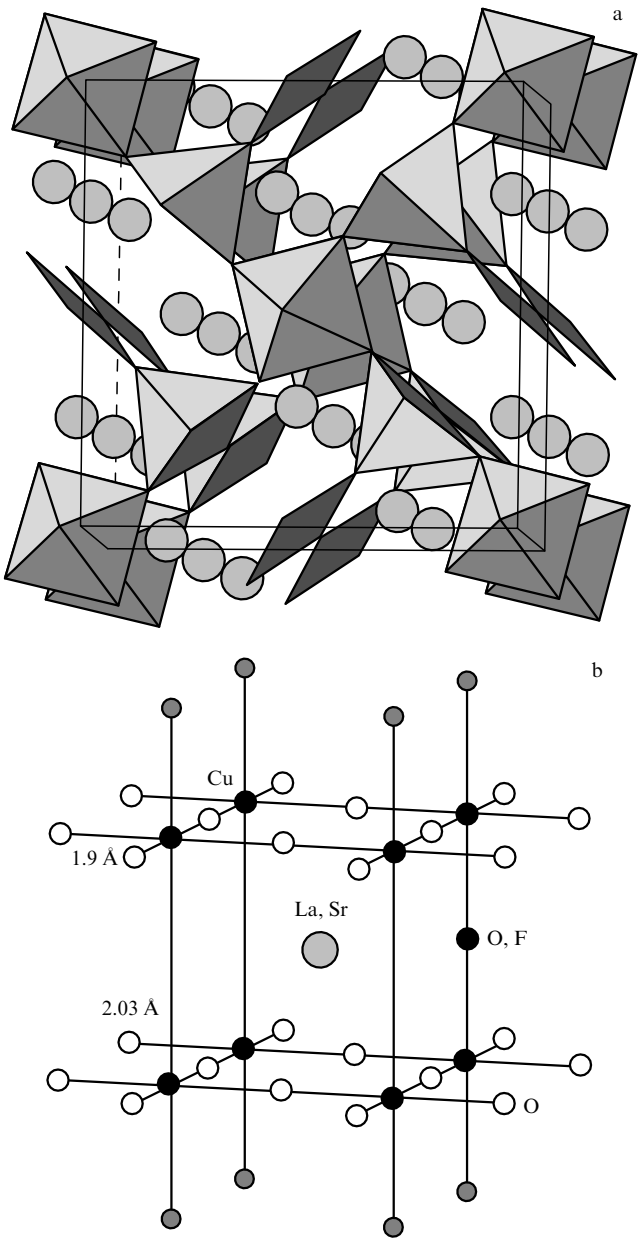

Figure 13. Schematic diagram of the structural transformation of $La_{6.5}Sr_{1.5}Cu_8O_{19.65}$ (a) into $La_{0.813}Sr_{0.187}Cu(O,F)_{3-\delta}$ (b) upon fluorination.

arrangement in the structure with alternating (CuO_2) and ($La_{0.85}Sr_{0.15}F$) layers. Such a compound could be an example of the simplest structure of superconducting cuprates.

For cuprates containing sodium chloride–type blocks, the ionic character of the $A-O$ bond leads to the fact that the strengths of the bonds in the $((R, A)O)$ layers are comparable to those of the bonds between neighboring $((R, A)O)$ layers. The structure of the Bi-containing layered cuprates $Bi_2Sr_2Ca_{n-1}Cu_nO_{2n+4+\delta}$ also contains (Bi_2O_2) blocks with a sodium chloride structure. In contrast to $((R, A)_2O_2)$ blocks with isotropic chemical bonds, only a weak van der Waals interaction is realized between layers in the (Bi_2O_2) block, which is related to the crystal-chemistry properties of the Bi^{3+} cation. The Bi–F bond is substantially ionic, which should result in a change in the structure of the (Bi_2O_2) layers with interstitial fluorine atoms.

The fluorination of the Bi-2201 $Bi_2Sr_{1.6}La_{0.4}CuO_{6.33}$ phase by XeF_2 causes the disappearance of incommensurate modulations (Fig. 14a), which indicates that interstitial fluorine changes the structure of the (Bi_2O_2) blocks [42]. Excess anions are placed in the interstices of the (Bi_2O_2) block, which are tetrahedrally coordinated by Bi atoms such that the (Bi_2O_2) block transforms into a ($Bi_2O_{2-x}F_{2+x}$) block in which Bi atoms are located in a single-cap square antiprism with four short Bi–F bonds and five long Bi–O bonds (Figs 14b–14d). Blocks with an analogous structure are encountered in representatives of the Aurivillius-phase homologous series, e.g., in Bi_2NbO_5F [43]. In the Bi-2201 phase, the (BiO) layers are almost flat and the distance between the Bi and O layers along the *c*-axis in these layers does not exceed 0.24–0.26 Å; but in the Aurivillius phase, this distance increases to 0.92–1.07 Å, leading to the 'splitting' of the (BiO) layer into two layers (one of which

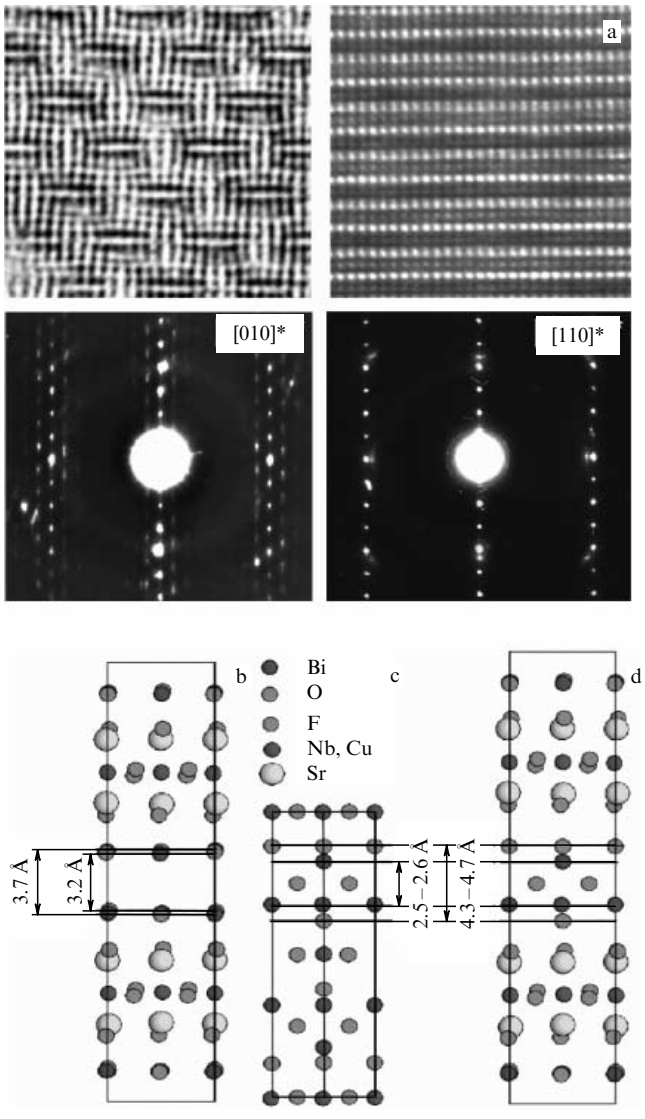

Figure 14. (a) High-resolution transmission electron microscopy images and electron diffraction patterns of the initial and fluorinated Bi-2201 phases, which indicate the disappearance of incommensurate modulations upon fluorination. The crystal structures of $Bi_2Sr_{1.6}La_{0.4}CuO_{6.33}$ (b) and Bi_2NbO_5F (c). (d) A model for the structure of the fluorinated tetragonal Bi-2201 phase.

consists of Bi atoms and the other of O atoms). An increase in the coordination number of bismuth in the fluorinated phase increases the Bi – O distances and the block size in the *ab* plane. As a result, the match is achieved between the $(Bi_2O_2F_2)$ blocks and (CuO_2) layers, which leads to the suppression of incommensurate modulations. We note that the fluorinated Bi – 2201 phase has a hybrid structure in which Bi-containing $(Bi_2O_{2-x}F_{2+x})$ blocks (as in the Aurivillius phases) and perovskite $A_2Ca_{n-1}Cu_nO_{2n+2}$ $(n = 1)$ blocks are matched; that is, such phases belong to the new family of cuprates $Bi_2A_2Ca_{n-1}Cu_n(O,F)_{2n+6}$, whose representatives can have superconducting properties.

8. Conclusions

In the last two decades of extensive studies of the superconducting properties of complex copper oxides, the possibilities of creating a new class of superconducting cuprates or further optimizing the properties of well-known compounds have been nearly exhausted. Nevertheless, it is too early to state that compounds with T_c higher than in the obtained values cannot exist among the complex cuprates. The increase in T_c in Hg-containing cuprates induced by an applied pressure or fluorination suggests that the chemical modification that causes a decrease in the in-plane $Cu-O_{plan}$ distance without changing the degree of folding the (CuO_2) layers is a promising way for increasing T_c in complex superconducting copper oxides. A simple isovalent cation substitution, which leads to isotropic compression of the structure, is likely to be ineffective. For example, a partial substitution of Sr for Ba atoms decreases T_c, since it is accompanied by a strong decrease in the axial Cu – O bond and the 'folding' of the (CuO_2) layer. A more promising way is thought to consist in the production of metastable layered structures using nontraditional chemical synthesis methods, such as the synthesis of epitaxial films using layer-by-layer deposition onto substrates with chosen lattice parameters, which can create anisotropic compression of the structure of a superconductor in the (*ab*) plane and artificial heterostructures exhibiting an analogous effect.

In this report, we demonstrated that the modification of the anion sublattice upon substituting halogen atoms (e.g., fluorine) for oxygen can modify the structure of complex cuprates to yield new compounds that can be potential high-temperature superconductors. Indeed, as can be seen from Table 3, complex copper oxofluorides often exhibit a T_c comparable to or higher than that of their oxygen analogues. An analogous example can be found among oxochlorides. The compound $(Sr,Ca)_3Cu_2O_{4+\delta}Cl_{2-y}$ has $T_c = 80$ K [44], which is well above the superconducting transition temperature of its oxygen analogue $La_{1.6}Sr_{0.4}CaCu_2O_{6+\delta}$ ($T_c = 60$ K). We note that the synthesis of such compounds requires the application and development of labor-intensive methods in order to produce a compound in its metastable state.

Table 3. Superconducting complex copper oxofluorides.

Oxofluoride	T_c, K	Oxygen analogue	T_c, K
$YBa_2Cu_3O_6F_2$	94	$YBa_2Cu_3O_{6.95}$	92
$Y_2Ba_4Cu_7O_{14}F_2$	62	$Y_2Ba_4Cu_7O_{14.92}$	80
$HgBa_2CuO_4F_{0.24}$	97	$HgBa_2CuO_{4.12}$	97
$HgBa_2CaCu_2O_6F_\delta$	128	$HgBa_2CaCu_2O_{6.22}$	127
$HgBa_2Ca_2Cu_3O_8F_\delta$	138	$HgBa_2Ca_2Cu_3O_{8+\delta}$	134
$Sr_2CuO_2F_{2+\delta}$	46	Sr_2CuO_3	—
$La_2CuO_4F_\delta$, $\delta \leqslant 0.18$	35 – 40	$La_2CuO_{4.032}$	38
$Nd_2CuO_{3.7}F_{0.3}$	27	$Nd_{2-x}Ce_xCuO_4$	24
$Sr_2CaCu_2O_{4.6}F_2$	99		
$Sr_2Ca_2Cu_3O_{6.2}F_{3.2}$	111		
$Sr_2Nd_{0.2}Ca_{0.8}Cu_2O_5F$	85		

References

1. Ginzburg V L *Phys. Lett.* **13** 101 (1964); *Zh. Eksp. Teor. Fiz.* **47** 2318 (1964); [*Sov. Phys. JETP* **20** 1549 (1965)]; *Usp. Fiz. Nauk* **174** 1240 (2004) [*Phys. Usp.* **47** 1155 (2004)]
2. Fomichev D V, D'yachenko O G, Mironov A V, Antipov E V *Physica C* **225** 25 (1994)
3. Attfield J P, Kharlanov A L, McAllister J A *Nature* **394** 157 (1998)
4. Kopnin E M et al. *Sverkhprovodimost'* **5** 530 (1992)
5. Cava R J et al. *Nature* **345** 602 (1990)
6. Kharlanov A L et al. *Physica C* **169** 469 (1990)
7. Cava R J et al. *Nature* **336** 211 (1988)
8. Khasanova N R et al. *Physica C* **190** 522 (1992)
9. Maeda H et al. *Jpn. J. Appl. Phys.* **27** L209 (1988)
10. Sawa H et al. *J. Phys. Soc. Jpn.* **58** 2252 (1989)
11. Wu M K et al. *Phys. Rev. Lett.* **58** 908 (1987)
12. Antipov E V, Abakumov A M, Putilin S N *Supercond. Sci. Technol.* **15** R31 (2002)
13. Aksenov V L et al. *Phys. Rev. B* **55** 3966 (1997)
14. Loureiro S M et al. *Physica C* **243** 1 (1995)
15. Radaelli P G et al. *Physica C* **216** 29 (1993)
16. Loureiro S M et al. *Physica C* **217** 253 (1993)
17. Antipov E V et al. *Physica C* **218** 348 (1993)
18. Van Tendeloo G et al. *Physica C* **223** 219 (1994)
19. Fukuoka A et al. *Phys. Rev. B* **55** 6612 (1997)
20. Zhang Q, Chen X *Physica C* **282 – 287** 905 (1997)
21. Scott B A et al. *Physica C* **230** 239 (1994)
22. Chu C W et al. *Nature* **365** 323 (1993)
23. Gao L et al. *Phys. Rev. B* **50** 4260 (1994)
24. Nuñez-Regueiro M et al. *Science* **262** 97 (1993)
25. Balagurov A M et al. *Phys. Rev. B* **59** 7209 (1999)
26. Hunter B A et al. *Physica C* **221** 1 (1994)
27. Aksenov V L et al. *High Pressure Res.* **14** 127 (1995)
28. Armstrong A R et al. *Phys. Rev. B* **52** 15551 (1995)
29. Aksenov V L et al. *Physica C* **275** 87 (1997)
30. Abakumov A M et al. *Phys. Rev. Lett.* **80** 385 (1998)
31. Cao Y et al. *Phys. Rev. B* **52** 6854 (1995)
32. Putilin S N et al. *Physica C* **338** 52 (2000)
33. Lokshin K A *Phys. Rev. B* **63** 064511 (2001)
34. Monteverde M et al. *Europhys. Lett.* **72** 458 (2005)
35. Wagner J L et al. *Phys. Rev. B* **51** 15407 (1995)
36. Locquet J-P et al. *Nature* **394** 453 (1998)
37. Abakumov A M, Rozova M G, Ardashnikova E I, Antipov E V *Usp. Khim.* **71** 442 (2002) [*Russ. Chem. Rev.* **71** 383 (2002)]
38. Kistenmacher T J *Phys. Rev. B* **36** 7197 (1987)
39. Shpanchenko R V et al. *Physica C* **280** 272 (1997)
40. Van Tendeloo G, Lebedev O I, Shpanchenko R V, Antipov E V *J. Electron Microsc.* **46** 23 (1997)
41. Abakumov A M et al. *J. Solid State Chem.* **149** 189 (2000)
42. Hadermann J et al. *J. Solid State Chem.* **156** 445 (2001)
43. Aurivillius B *Ark. Kemi* **4** 39 (1952)
44. Jin C-Q et al. *Nature* **375** 301 (1995)